BOLLETTINO DI GEOFISICA TEORICA ED APPLICATA VOL. XXXII, N. 126 - JUNE 1990

C. BRAITENBERG and M. ZADRO

THE MAGNETOTELLURIC CAMPAIGN IN EASTERN ALPS, NE-ITALY: REGIONAL AND LOCAL 2-D RESPONSES OF THE SEISMIC ZONE

Abstract. The one year long measurements of one telluric (T) and two magnetotelluric (MT) stations in the seismically active Friuli region, NE-Italy are studied in the frequency range from 3 cpm (cycle per minute) to one cph (cycle per hour) in order to investigate both the deep structure electric response as well as the precursory earthquake phenomena. Normal features and mutual relations of the magnetotelluric (MT) field recorded in the three stations are studied. From the data of the two MT-stations, the impedance is calculated by an iterative, signal-to-noise enhancing method for different time sequences throughout the year of observation. Impedance is analyzed in a non-typical manner for MT-studies producing, next to two apparent resistivities and phase values, the orientation and ellipticity of the singular elliptically polarized state of the magnetic (B)- and T-field, thus describing the impedance fully. The polarization of the B- and T- fields as well as the impedance are computed, which show particular regional characteristic tied to deep structures. The influence of an earthquake of magnitude 4.2 which occurred on February 1, 1988, during the measuring campaign within a distance of 40 km from all three stations, is studied, but no anomalous effect has been detected in the analysis.

INTRODUCTION

The observation of changes correlated to seismic events in resistivity or in the T-field has been reported by several authors, for instance Myachkin et al. (1972), Qian (1984), Sobolev (1975), Varotsos and Alexopoulos (1984), Yamazaki (1975). The time scales and amplitudes of the observed variations are very different, as are their magnitudes. With the aim of detecting such anomalous features in the seismically active Friuli region (NE-Italy), a MT-campaign was set up in collaboration with the Polish Academy of Sciences.

Friuli is characterized by two main strike directions: the Alpine, E-W oriented and the Dinaric, NW-SE oriented. The campaign, which was operative from July 1987 to June 1988, included two MT-stations and one T-station. The MT-stations were sited on a purely Alpine (Forni di Sotto-FDS) and purely Dinaric (Iainich-IAI) environment respectively, whereas the T-station (Villanova-VIL) was sited in a region where the two strike-directions meet (Fig. 1). For an analysis of the data based on a one component impedance calculation and a one-dimensional inversion, see Zadro et al. (1988), and for the detection of an anomalous T- field correlated with seismicity, see Zadro et al. (1990).

In the present analysis, the MT 2-component data are revised taking into account several time sections under different conditions (high magnetic activity, low magnetic activity, earthquake occurrence). There are two aims to the research:

a) the detection of normal regional 2- and 3-D features of the field and their relation to deep structures (polarization of the B- and T- fields and resistivity).

b) the detection of anomalous features and their relation to seismicity by studying the time

Manuscript received May 31, 1990; accepted June 25, 1990.

Istituto di Geodesia e Geofisica, University of Trieste, 34100 Trieste, Italy.

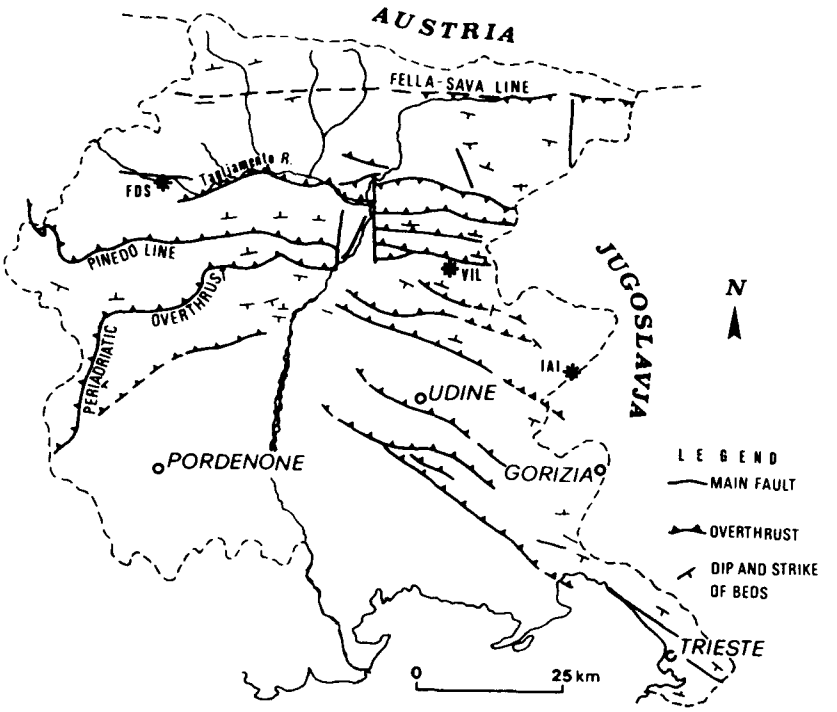

Fig. 1 - Map of the Friuli seismic area (after Slejko et al., 1987). The positions of the two MT-stations Iainich (IAI) and Forni di Sotto (FDS) and of the T-station Villanova (VIL) are indicated.

changes in impedance for an earthquake of magnitude greater to or equal 4. The example under consideration is of an earthquake that occurred within 40 km of all stations.

INSTRUMENTATION

The two MT-stations FDS (Lat 46°23'N, Long 12°40'E) and IAI (Lat 46°06'N, Long 13°33'E) were each equipped with a three- component Torsion-Photoelectric Magnetometer (Jankowski et al., 1984) and a T-recording system consisting of two 50-100 m long electric lines, one oriented N-S and the other E-W. The vertical magnetic component will not be used in the following as it was severely affected by interruptions and breakdowns. The T-station VIL (Lat 46°15'N, Long 13°17'E) was only equipped with the T-recording system. The digital data were recorded on magnetic tape at a 20 second sampling interval.

DATA SELECTION

In the Table the time sections analyzed are listed. In the Table, distinction has been made between cases of high and low magnetic activity, which is important for further analysis, as it will be shown that the measurements made during low magnetic activity are predominantly influenced by man-made MT-sources. The occurrence of an earthquake of magnitude M=4.2 (the most intense during the campaign) with epicentre (Lat 46°13'N, Long 13°02'E) 20 km west of station VIL (34 km from FDS and 41 km from IAI, respectively) and at shallow depth (h=5km) coincides with a period of low magnetic activity. Fig. 2 shows an example of the measurements taken at the three stations during high (Fig. 2a) and during low (Fig. 2b) magnetic activity. Observation of the B-field in Fig. 2b reveals a field of high frequency content at station

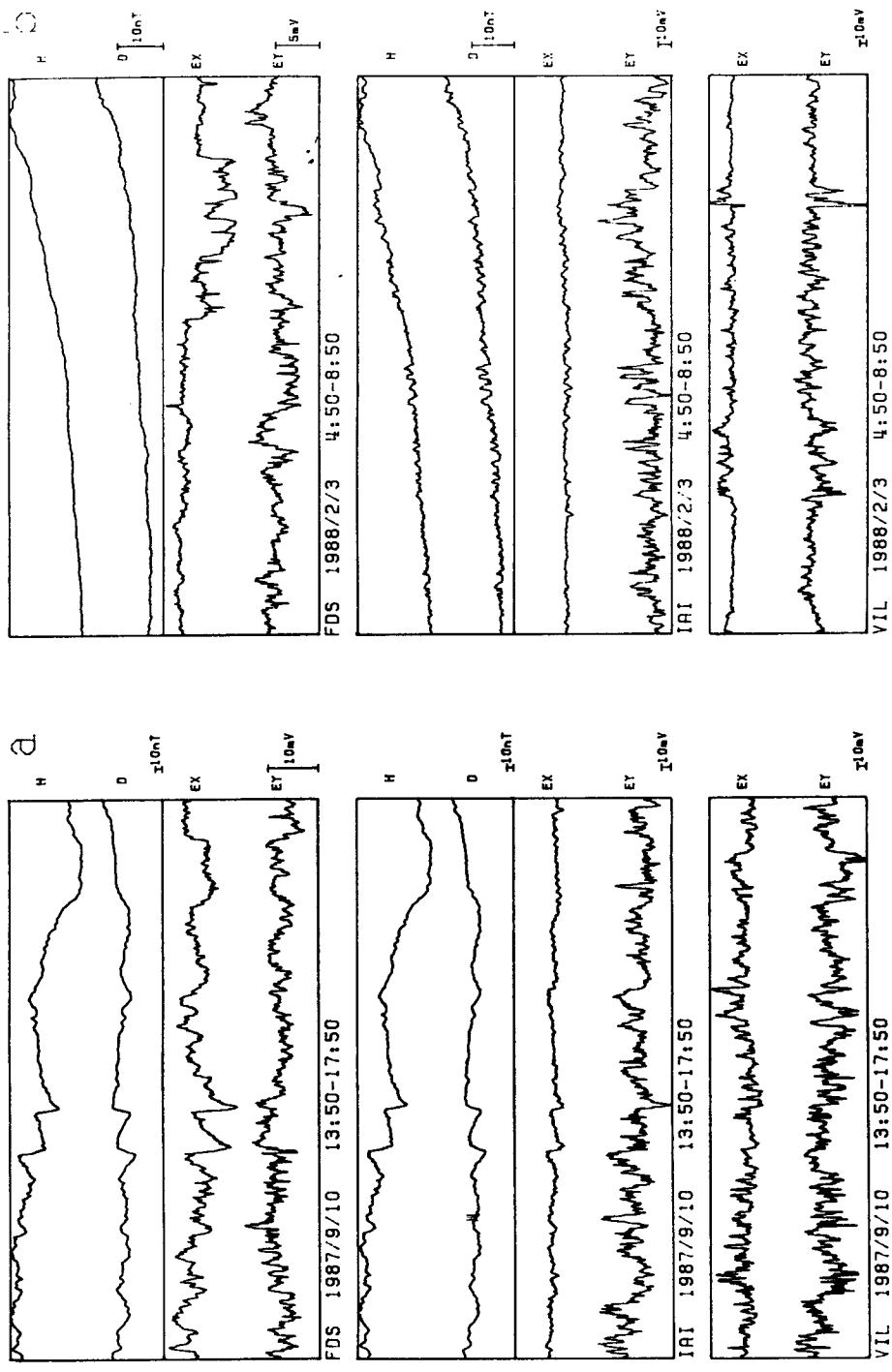

Fig. 2 - T- (Ex, Ey) and B-field (H, D) recorded at the MT- stations FDS, IAI and the T- station VIL over a time interval of 4 hours. H and Ex are aligned north, D and Ey eastwards.
a) During a period of high magnetic activity.
b) During a period of magnetic quiesoence.

IAI which is not present at station FDS, but is well correlated with the T-fields recorded in IAI and VIL.

Table-Time sections selected for the analysis.

a) **High magnetic activity:**
1) 28 h during: (7 Sept. 1988 to 20 Sept. 1987)
2) 26 h during: (14 Jan. 1988 to 15 Jan. 1988)
3) 26 h during: (21 Feb. 1988 to 22 Feb. 1988)

b) **Low magnetic activity:**
Period of earthquake occurrence (M=4.2, 1. Feb. GMT 14:20, 1988)
1) 24 h during: (27 Jan. 1988 to 3 Feb. 1988).

POLARIZATION OF DATA

The polarization of the T- and B-fields is analyzed with the aim of finding relationships with geological and/or seismotectonic features. A measure of polarization is obtained from the direction of the major axis and the ellipticity (one minus ratio of minor to major axis) of the distribution ellipse of the 2-D, T- and B-field vectors calculated for a certain time interval.

The polarization directions of the T- and B-field are calculated for 12 time intervals, each 4 hours long, recorded during 3 magnetic storms, respectively, in the months of September, January and February. The time sections were chosen during high B-field activity in order to have high level signals, thus minimizing noise contributions. For each interval of high B-field activity indicated in the Table, 4 time sections, each 4h long, are selected. Frequency dependence is allowed for by band filtering the data on the three distinct frequency bands (a) (1/50 - 1/6 cpm), (b) (1/5 - 1/4 cpm), (c) (1/3-1/2 cpm).

In the Fig. 3, the polarization directions of the B- and T- field respectively, (directions of the major axis of the distribution ellipse) are graphed separately for each station and frequency bands. For the B-field (Fig. 3a), the ellipticity values (not depicted) are about .5; thus over an interval of 4 hours, the direction is generally well defined. Although a high dispersion of the orientations can be observed, a preferential direction of roughly N30W-S30E appears mostly at the higher frequencies. The orientation of the B-field seems little affected by the directions of the structural surface lineaments at the two stations and thus seems tied to inhomogeneities on a larger scale, which must affect deep structures.

Compared with the B-field, the direction of the T-field (Fig. 3b) is highly dependent on the observation site and varies mostly in space, thus revealing high sensibility to the local structure. The polarization is well defined showing high ellipticity values of up to .8 (not drawn). Summarizing the polarization values of the T-field, we find that generally two preferential orientations appear, one, though, being dominant over the other. The mean orientations are:

	FDS	IAI	VIL
for low frequencies:			
Dominant:	N40W-S40E	N80E-S80W	N70W-S70E
Secondary:	N80W-S80E	N40E-S40W	
for high frequencies:			
Dominant:	N70W-S70E	E-W	N70W-S70E
Secondary:	N50W-S50E	N-S	

Secondary orientations concern shorter polarization axes. The polarization axis at VIL is very stable, regardless of both intensity and frequency.

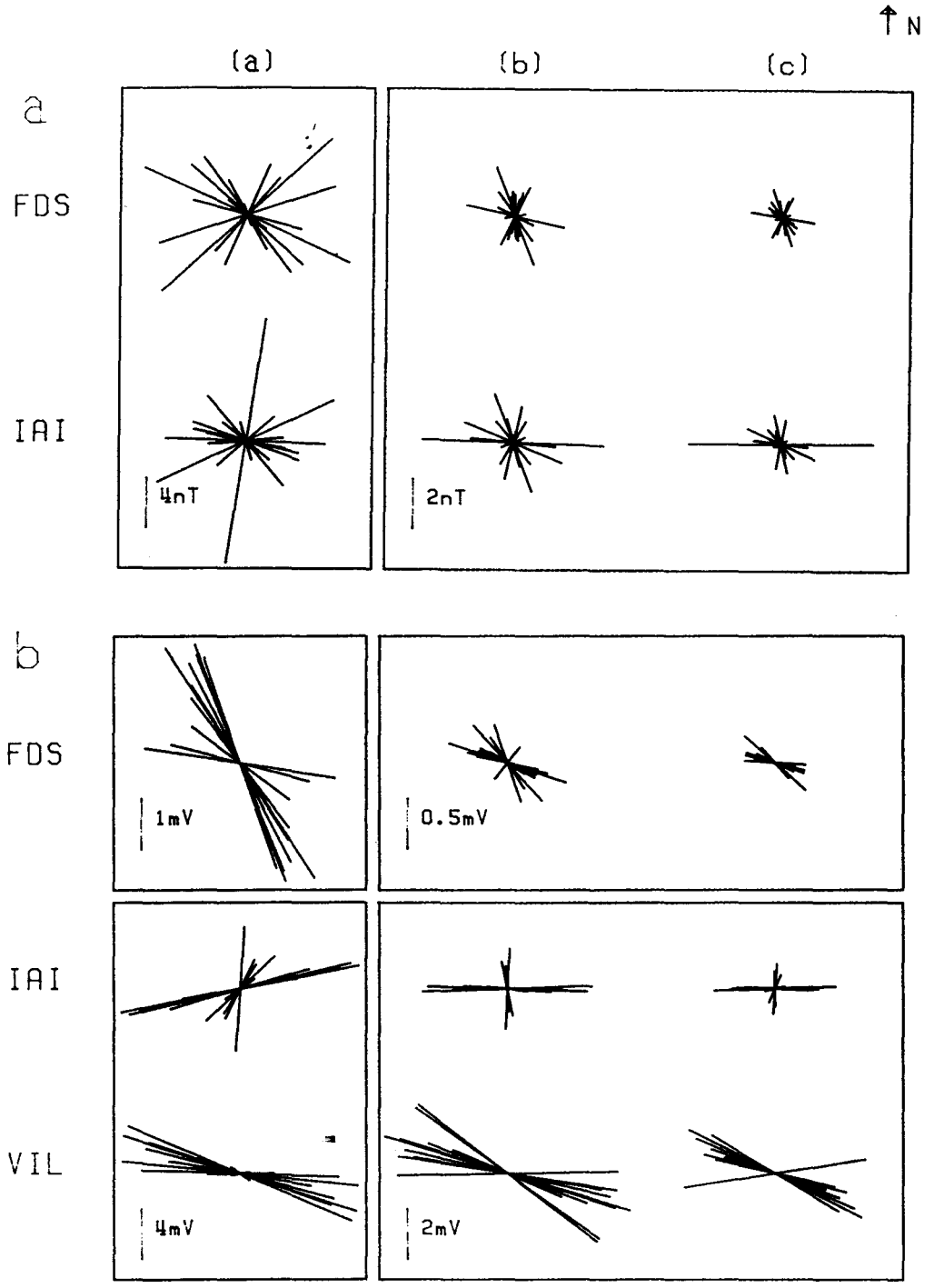

Fig. 3 - Polarization direction of B- and T-field for 12 subperiods each of 4 h length recorded during high magn. activity in September, January and February. The three columns (a), (b), (c) refer to the frequency bands (1/50 - 1/6 cpm), (1/5 - 1/4 cpm), (1/3 - 1/2 cpm), respectively.
a) B-field for the MT-stations FDS and IAI.
b) T-field for the MT- stations FDS, IAI and the T-station VIL.

In an ideal 2-D model, the T-field should be polarized in a direction orthogonal to the structural lineaments. Moreover, the higher the electric field frequencies, the more the superficial layers should be involved. By considering the dominant responses, it results that, at tens of km of depth, the structures should be oriented as follows: N50E-S50W at FDS, N10W-S10E at IAI and N20E- S20W at VIL. At shallower depths, a counterclockwise rotation of 30° and a clockwise rotation of 10° is detected at FDS and IAI respectively, whereas VIL maintains the same orientation. Of course, lateral inhomogeneities can greatly modify the 2-D assumption.

LINEAR RELATIONSHIP BETWEEN T- FIELDS MEASURED AT TWO STATIONS

Neglecting a phase-shift between the spectral components of the T-fields measured at two stations, and assuming the linear relationship between the fields to be constant over a chosen frequency interval, the 2x2 real square matrix **K** which maps the horizontal components of the T-field $\mathbf{e}_a(t)$ to those $\mathbf{e}_b(t)$ in stations 'a' and 'b' is calculated by minimizing the quantity $<(\mathbf{e}_b(t)-\mathbf{K}\,\mathbf{e}_a(t))^2>$ (here $<\ldots>$ indicates the mean value over a certain time interval), where $\mathbf{e}_a(t)$ and $\mathbf{e}_b(t)$ are filtered over the frequency band in question.

A Singular Value Decomposition (SVD) (Golub and Van Loan, 1983; Yee and Paulson, 1987b) of the matrix **K** is applied to obtain the singular values τ_1, τ_2, the product d of which (the value of the determinant) can be set in relation to the principal restitivities $\varrho_{a1,2}$ $\varrho_{b1,2}$ and gives the ratio of the geometric mean of the principal resistivities at the two stations (see Eq. (7) in the following paragraph):

$$|d| = |\tau_1 * \tau_2| = \left[\frac{\varrho_{b1} * \varrho_{b2}}{\varrho_{a1} * \varrho_{a2}}\right]^{1/2}. \tag{1}$$

The values for the determinant of the linear relationship between the T-fields measured at two stations, for the four frequency bands (a) (1/240 - 1/27 cpm), (b) (1/24 - 1/13 cpm), (c) (1/12 - 1/8 cpm), (d) (1/8 - 1/6 cpm), during high magnetic activity in September, are given in the following:

(st. 1: input field, st. 2: output field)

st.1 - st.2	(a)	(b)	(c)	(d)
FDS-VIL:	30	30	40	70
FDS-IAI:	5	6	8	15
IAI-VIL:	6	5	5	5

It is seen that, generally, the higher values pertain to higher frequencies. The highest resistivities are found in VIL and the lowest in FDS. This show that the electric signals in FDS are very weak over the entire frequency band, thus reducing the reliability of the telluric results obtained from that station, whereas the best results should be obtained at VIL.

IMPEDANCE AND DERIVED QUANTITIES

In a Cartesian coordinate system the 2-D horizontal-plane impedance **Z(f)** of the structure is defined by:

$$\mathbf{e(f)} = \mathbf{Z(f)}\ \mathbf{b(f)}, \tag{2}$$

where **Z(f)** is a complex 2x2 matrix and **e(f)**, **b(f)** are the horizontal components of the T-and

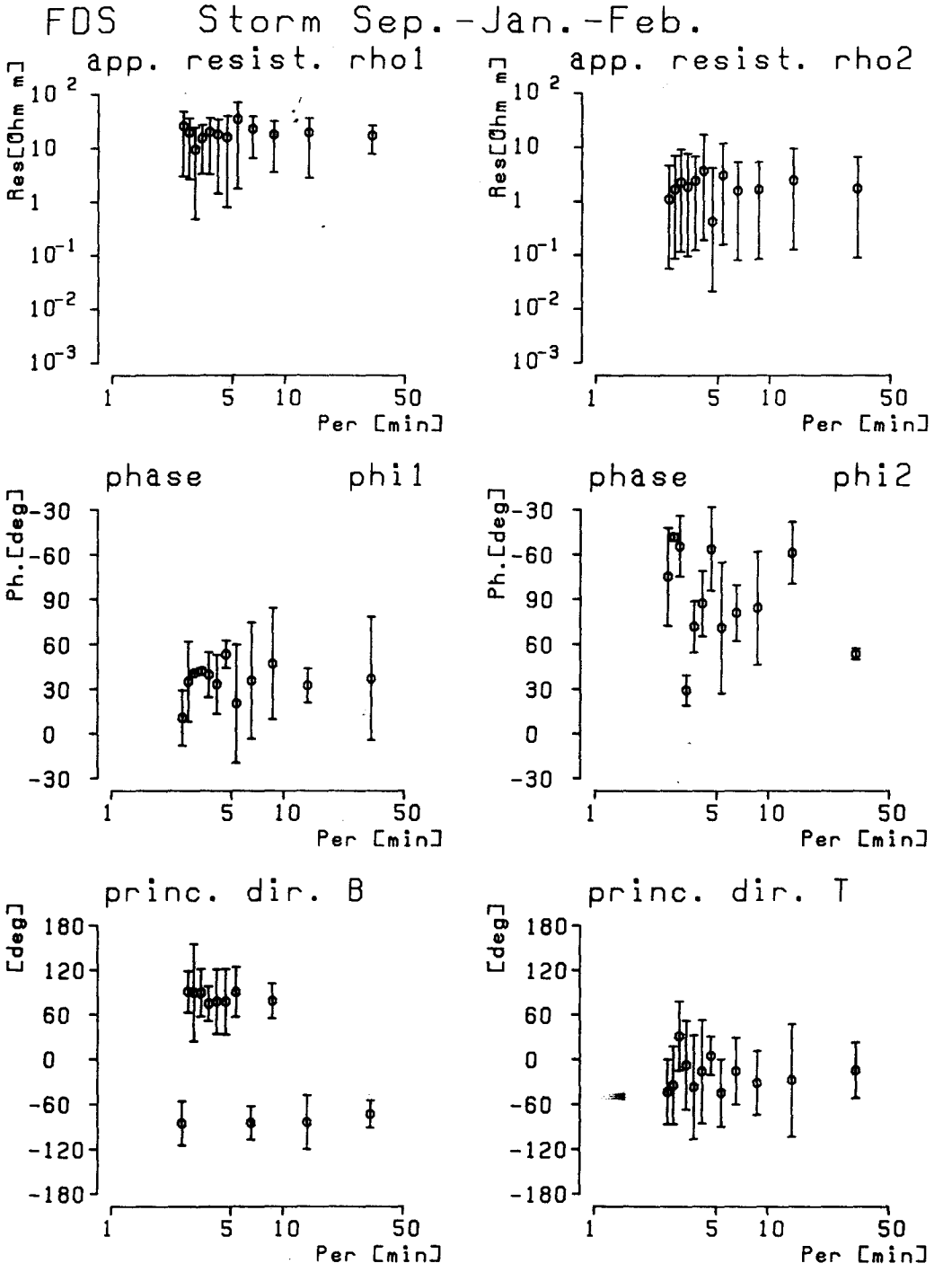

Fig. 4 - Station FDS: Mean impedance calculated for periods in September, 1987, mid January and end of February, 1988. Impedance decomposed into major and minor principal resistivities and corresponding phases (res1, phi1), (res2, phi2) and principal directions and ellipticity of B- and T- field.

B-field, respectively, in frequency space. The computation of **Z(f)** is accomplished with an iterative, signal-to-noise enhancing method explained in Appendix 1. Impedance is analyzed by a method (La Torraca et al., 1986; Yee and Paulson, 1987a) which with 8 independent parameters fully describes the calculated matrix. The method does not set any requirements either on the degree of complexity of the underlying structure or on the inducing source, and is very convenient to our purpose of detecting time changes in impedance. We apply the complex SVD of **Z(f)** (see Appendix 2) obtaining the following parameters:

complex singular values:	μ_1, μ_2
principal direction B-field:	α
ellipticity B-field:	e
principal direction T-field:	β
ellipticity T-field:	h

Then we introduce the following derived quantities:

principal resistivities	principal phases
$\varrho_1 = .2P\,\lvert\mu_1\rvert^2$	$\phi_1 = \text{argument}\,(\mu_1)$
$\varrho_2 = .2P\,\lvert\mu_2\rvert^2$	$\phi_2 = \text{argument}\,(\mu_2)$,

where P is the period in seconds. The B-field is measured in nT, the T-field in mV/km and the resistivity in Ohm m. The above parameters allow the following interpretation: the application of impedance **Z(f)** on an elliptically polarized state of the B-field at frequency f, orientation α, ellipticity e and unit amplitude results in a polarized state of the T-field, with orientation β and ellitpicity h, phase shifted by ϕ_1 and with field amplitude $|\mu_1|$. The same polarized state of the B-field, but with orientation $\alpha+90°$ results in a T-field with orientation $\beta+90°$, ellipticity h, phase shifted by ϕ_2 and with field amplitude $|\mu_2|$.

In the case of a 2-dimensional structure with constant resistivity in one horizontal direction and a plane-wave impiging on the earth-surface (Cagniard's assumption), the strike direction, dimensionality and principal impedances becove evident from the parameters. The impedance for the horizontal components of an impinging plane wave is (Kaufmann and Keller, 1981):

$$\mathbf{Z} = \begin{bmatrix} \sin 2\alpha\,(z_1+z_2)/2 & z_1\cos^2\alpha - z_2\sin^2\alpha \\ z_2\cos^2\alpha - z_1\sin^2\alpha & -\sin 2\alpha\,(z_1+z_2)/2 \end{bmatrix}, \tag{4}$$

where z_1, z_2 ($|z_1| > |z_2|$) are the complex principal values with phase equal to 45°, and where the coordinate system is rotated by the angle α with respect to the direction of structure. By applying SVD we obtain:

principal direction B-field: α
principal direction T-field: $\alpha+90°$
singular values: $\mu_1 = z1$, $\mu_2 = z2$

With the above decomposition of **Z(f)**, we can show how the determinant of the complex 2x2 matrix **K(f)**, which maps the horizontal components of the T- field in station 'a' to those in station 'b' (in frequency space), is related to the ratio of the resistivities at the two sites. Assuming a common inducing B-field in the two MT-stations, the relation between the impedances is $\mathbf{Z}_b(f) = \mathbf{K}(f)\,\mathbf{Z}_a(f)$, with $\mathbf{Z}_a(f)$, $\mathbf{Z}_b(f)$ the impedances at station a and b. On applying SVD and calculating determinants we obtain:

$$\mu_{b1}^*\,\mu_{b2} = \tau_1^*\,\tau_2^*\,\mu_{a1}^*\,\mu_{a2}, \tag{5}$$

where the μ_a, μ_b and τ are the singular values of $\mathbf{Z}_a(f)$, $\mathbf{Z}_b(f)$ and **K(f)**, with notations as in the previous paragraphs. By taking moduli we obtain:

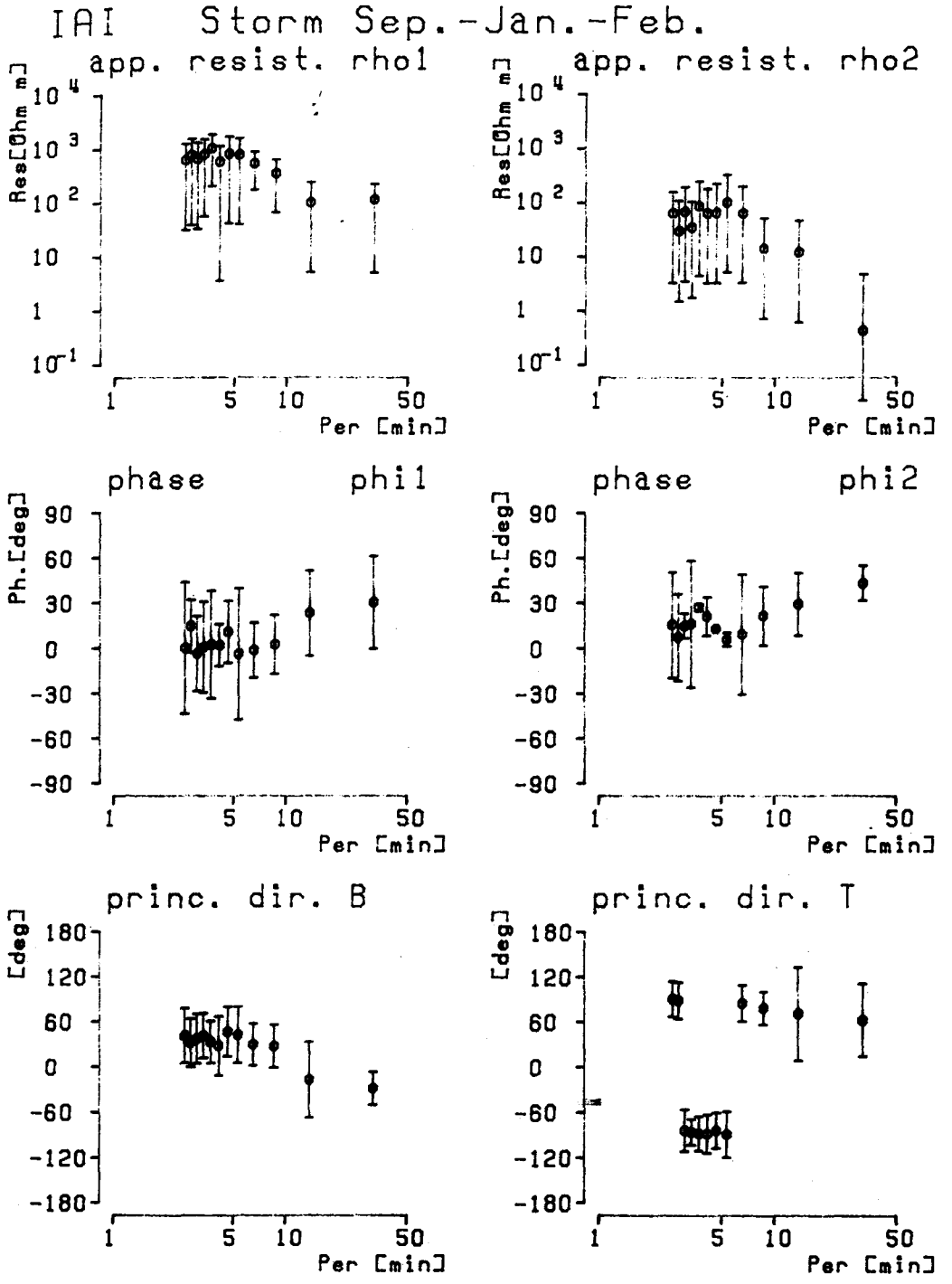

Fig. 5 - Station IAI: Mean impedance calculated for periods September, 1987, mid January and end of February, 1988. The decomposition of impedance as in Fig. 4.

$$|\tau_1 * \tau_2| = \frac{|\mu_{b1} * \mu_{b2}|}{|\mu_{a1} * \mu_{a2}|} \tag{6}$$

which, with the above definition for apparent resistivity, leads to the relation (see previous paragraph) that the modulus of the determinant of **K(f)** is equal to the ratio of the geometric means of the two principal resitivities in the two stations:

$$|\tau_1 * \tau_2| = \left[\frac{\varrho_{b1} * \varrho_{b2}}{\varrho_{a1} * \varrho_{a2}} \right]^{1/2}, \tag{7}$$

Eq. (7) is an extension to an arbitrary structure of the frequently used relation in telluric studies, valid only for a 2-D structure (Yungul, 1977):

$$|\tau_1 * \tau_2| = \left[\frac{\varrho_b}{\varrho_a} \right]^{1/2}, \tag{8}$$

where ϱ_a, ϱ_b are the apparent resistivities at the sites 'a', 'b' for the polarization state of the T-field orthogonal to the strike direction.

In Figs. 4 to 6, the results obtained for the magnetic storm activity (Figs. 4 and 5) and the seismic activity (Fig. 6) for the two MT-stations are presented. Impedance is calculated for 12 equispaced frequencies which range from 1/35 cpm to 1/2.6 cpm, and the 8 quantities obtained from the decomposition of impedance (2 principal resistivities and associated phase values, and the principal direction and rotation angle of the real and imaginary parts of the impedance) are graphed. All angles are measured clockwise, the angle defining the principal direction indicating deviation from North. We thus maintain all information contained in the impedance, and a change in the electrical resistivity structure may be observed as a variation of the parameters, and can thus be qualitatively ascertained.

HIGH MAGNETIC ACTIVITY

The results for the periods of high magnetic activity in September, January and February are depicted in Figs. 4 and 5 for stations FDS and IAI, respectively. Error-bars indicate one standard deviation of each parameter, as calculated by error-propagation using the standard deviation from the weighted mean of the components of impedance calculated in 12 subperiods each of 4h length. The weights are given by the signal-to-noise ratio (SNR) of the T- field for each subperiod and frequency band defined by:

$$SNR = \frac{\langle |\mathbf{Z(f)\ b(f)}|^2 \rangle}{\langle |\mathbf{e(f) - Z\ b(f)}|^2 \rangle}, \tag{9}$$

where $\langle \ldots \rangle$ indicates the mean value over the frequency band.

As the variation of the impedance values obtained during the three magnetic storms did not exceed the error-bars, we only present in the figures above (Figs. 4 and 5) the mean over the three periods analysed, and conclude that no significant variation of impedance was observed for the time from September to the end of February. Consequently a long term effect due to the earthquake of M=4.2 which occurred on February 1 was not observed.

For station FDS (Fig. 4), the order of magnitude of the principal apparent resistivity is a few tens of Ohm m and a few Ohm m for ϱ_1 and ϱ_2, respectively. Phase values are about 30°. Principal directions of the B-field are mostly E-W, whereas for the T-field, we find N50W. The ellipticity values obtained are not graphed, as the scattering was very high and no typical ellipticity values emerged.

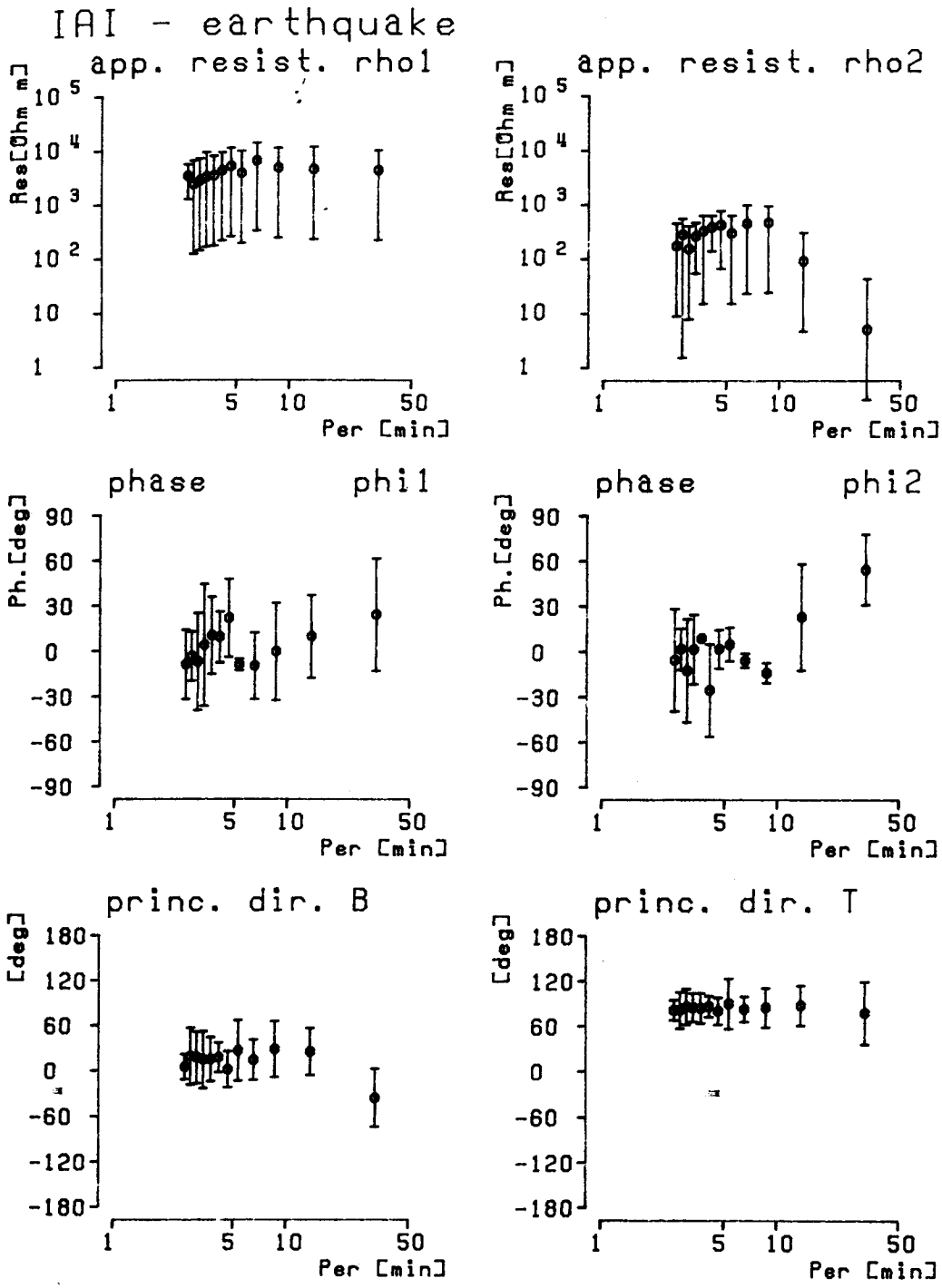

Fig. 6 - Station IAI: Mean impedance calculated for period January 27 to February 3, 1988. The decomposition of impedance as in Fig. 4.

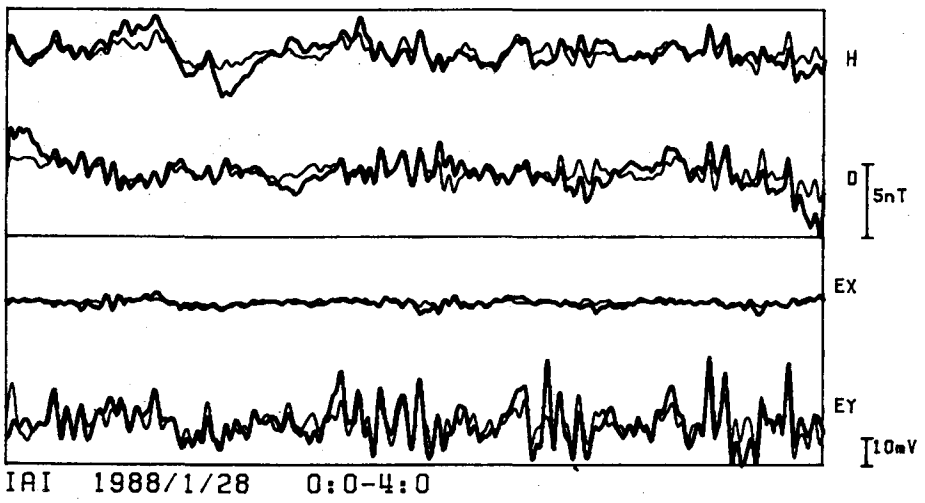

Fig. 7 - Graphical superposition of recorded (thick line) and signal-to-noise ratio enhanced (thin line) T- and B-fields. Station IAI over 4 hour time interval during period of low magnetic activity.

For station IAI (Fig. 5) the apparent resistivity values are about 700 Ohm m and 70 Ohm m for ϱ_1 and ϱ_2 respectively. Phase values are very low, but better defined than at FDS. The principal direction of the B-field is about N30E, whereas we find a very definite E-W orientation for the T-field. The ellipticity values for the T-field show a high degree of polarization of the field (greater than or equal to .8).

LOW MAGNETIC ACTIVITY

An MT-field, with regional extension of at least 30 km and stable characteristics, emitted from a presumably man-made artificial source is revealed by stations IAI and VIL (Fig. 2b). Since with these fields, the Cagniard assumption of impinging plane waves is violated, a different impedance must be expected for an unchanged underlying structure. This effect apart, a short-time change in the structure should emerge from the impedance parameters, given the condition of a stable MT-source during the time in question. During seismically active time-periods, but lacking a strong natural MT-field, this field is used for impedance calculations.

The results of mean impedance calculations at station IAI for the 10 days of low magnetic activity, including the time of the earthquake occurrence, are presented in Fig. 6. As no significant variation was observed over the period of analysis, we conclude that any effect of the earthquake on resistivity structures, as detected by impedance calculations, was below resolution power. Comparison with Fig. 5 shows the diverse sounding curves, due to the source effect, which emerge in the apparent resistivity values (almost a factor 10 on the whole frequency band) and in the principal direction of the B-field (difference of about 30°).

In Fig. 7, the graphical superposition of the recorded and calculated (with impedance and admittance) MT-field is given, for a 4h-period during low magnetic activity. A good agreement between the two fields is seen.

CONCLUSIONS

An analysis of the 9-month long recordings of the MT-campaign from two MT-stations and one T-station gave various results in a region where MT-studies have never before been accomplished. The data were analysed over the frequency range from 1/3 to 1/50 cpm, the higher value being limited by the 20 s sampling. In accordance with this frequency range, the

results should be determined by the deep resistivity structures, rather than the local ones.

Polarization studies show that the T-field has a very well defined preferential direction, weakly dependent on frequency, which, however, varies greatly from station to station. The preferential direction of the B-field is much less defined and differs little from stations FDS to IAI. The polarization of the T-field may be connected to the different structural alignments present beneath the stations, whereas the preferential direction of the B-field must be determined by inhomogeneities on a much greater scale.

Principal impedance values together with principal directions and ellipticity values are obtained from the complex SVD of the calculated impedance matrix, a convenient method to use in a tectonically complicated region such as the Friuli. Usually in MT-studies, the principal impedance values are set equal to the off-diagonal elements of the calculated impedance matrix, with the reference system being aligned to the strike direction (see Eq. 4). This procedure, however, is only correct if the underlying structure can be modelled in 1-D or 2-D and hence is not adequate in our case. Due to the presence of noise in the data, an iterative, signal-to-noise enhancing method is used for calculating impedance. The duration of the campaign allowed the selection of the data for the apparent resistivity determination exclusively during periods of high magnetic activity, thus reducing the artificial noise contribution to a minimum. The apparent resistivity values in IAI are greater than those in FDS by a factor 100. The principal direction fo the T-field obtained from SVD of impedance confirms the polarization directions found in the polarization study.

Lastly, we looked for impedance changes connected to a $M=4.2$ earthquake which occurred within 40 km of the three stations. The time variation of impedance was looked for on 1) the long term (several months) and 2) the short term (10 days) for both MT-stations FDS and IAI. The earthquake occurred during a magnetic low, but for the short-time analysis, we succeeded in exploiting a non-Ionospheric field owing to the fact that the field of a stable source was individualized. The problem that the calculated impedance not only is structure but also source-type dependent is overcome as we seek for relative changes of impedance only. In both stations any variation of impedance connected to the seismic event was below resolution power.

Acknowledgements. We wish to thank Prof. V. Iliceto and Dr. G. Santarato for their careful reading of the manuscript, and G. Cavicchi for help in drawing the figures.

APPENDIX 1

ITERATIVE METHOD

The iterative method is preferable to the simple least squares method (lsm) in the presence of noise on both the B-and T- fields as otherwise the calculated impedance $\mathbf{Z(f)}$ will be biased. For a similar approach, see also Kao and Rankin (1977). With $\mathbf{m}_0(\mathbf{f})$, $\mathbf{b}_0(\mathbf{f})$, the Fourier transforms of the T- and B-field measurements, $\mathbf{Z}(\mathbf{f})_n$, $\mathbf{Q}(\mathbf{f})_n$ the impedance and admittance, $\mathbf{m}_n(\mathbf{f})$, $\mathbf{b}_n(\mathbf{f})$ the signal enhanced T- and B-fields, all at the n-th step, the iteration process is defined by:

graph 1:

from condition:
$\sigma^2 = \langle |\mathbf{m}_{n-1}(\mathbf{f}) - \mathbf{Z}(\mathbf{f})_n \mathbf{b}_{n-1}(\mathbf{f})|^2 \rangle =$ min calculate $\mathbf{Z}(\mathbf{f})_n$ and the predicted T-field:
$\mathbf{m}_n(\mathbf{f}) = (1-q)\mathbf{m}_{n-1}(\mathbf{f}) + q\, \mathbf{Z}(\mathbf{f})_n \mathbf{b}_{n-1}(\mathbf{f})$
from condition:
$\sigma^2 = \langle |\mathbf{b}_{n-1}(\mathbf{f}) - \mathbf{Q}(\mathbf{f})_n \mathbf{m}_n(\mathbf{f})|^2 \rangle =$ min calculate $\mathbf{Q}(\mathbf{f})_n$ and the predicted B-field:
$\mathbf{b}_n(\mathbf{f}) = (1-q)\mathbf{b}_{n-1}(\mathbf{f}) + q\, \mathbf{Q}(\mathbf{f})_n \mathbf{m}_n(\mathbf{f})$
substitute n with n+1

(With the simbol $\langle \ldots \rangle_i$ we denote the mean value over the spectrum.)

Factor q is a weighting factor that lies between 0 and 0.5 which determines the effectiveness of each iteration step.

Next, we show that the process is signal-to-noise ratio enhancing. We separate the signal from the noise for the T- and B-field:

$$\begin{aligned} \mathbf{m}(\mathbf{f}) &= \mu(\mathbf{f}) + \mathbf{r}(\mathbf{f}) \\ \mathbf{b}(\mathbf{f}) &= \beta(\mathbf{f}) + \mathbf{s}(\mathbf{f}), \end{aligned} \tag{1}$$

where r(f), s(f) are the Fourier transforms of the noise r(t), s(t) and where the fields $\mu(f)$, $\beta(f)$ are linearly related by the impedance $Z(f)_0$:

$$\mu(f) = Z(f)_0\, \beta(f), \tag{2}$$

where

$$Z(f)_0 = \begin{bmatrix} z_{11} & z_{12} \\ z_{21} & z_{22} \end{bmatrix}.$$

The relationship between $\mathbf{Z(f)}_1$ calculated at the first iteration step and impedance $\mathbf{Z(f)}_0$ is:

$$Z(f)_1 = Z(f)_0 \begin{bmatrix} t & s_1 \\ s_2 & t \end{bmatrix}, \tag{3}$$

where the values of t, s_1 and s_2 depend on the signal-to-noise ratio, polarization and coherence of the components of the B-field. The factor t varies between 0 and 1 and approximates the value 1 for increasing SNR of the measured B-field.

Under the condition of low coherence between the components of the B-field, the relation (3) reduces to:

$$Z(f)_1 \approx t\, Z(f)_0 \tag{4}$$

Thus, the calculated impedance values are systematically too small in amplitude whereas little distortion of the matrix is present.

In the case that relation (4) holds, at the n-th iteration step it holds:

$$\mathbf{m}_n(\mathbf{f}) \approx x_n\, \mu(\mathbf{f}) + y_n\, \mathbf{r}(\mathbf{f}) + z_n\, \mathbf{Z}(\mathbf{f})\, \mathbf{s}(\mathbf{f}) \tag{5a}$$

$$\mathbf{b}_n(\mathbf{f}) \approx x_n' \beta(\mathbf{f}) + z_n'\, \mathbf{Q}(\mathbf{f})\, \mathbf{r}(\mathbf{f}) + y_n'\, \mathbf{s}(\mathbf{f}). \tag{5b}$$

The factors x_n, y_n, z_n, x_n', y_n', z_n', can be named:

x_n, x_n' - *signal factor*

y_n, y_n' - *noise factor*

z_n, z_n' - *contamination factor.*

Assuming further that the SNR and coherence are approximately equal for the components of the el. and magn. fields, we find that:

$$\begin{aligned} x_n &\approx 1 \\ y_n &\approx 1-nq \\ z_n &\approx nq. \end{aligned} \tag{6}$$

The SNR for the n–th iteration is:

$$\Gamma_n = \frac{x_n^2 |\mu|^2}{y_n^2 |r|^2 + z_n^2 |Zs|^2} \tag{7}$$

inserting the values obtained in (6):

$$\Gamma_n \approx \frac{|\mu|^2}{(1-qn)^2 |r|^2 + (qn)^2 |Zs|^2} \tag{8}$$

From (8) can be seen that the SNR increases at every iteration step under the condition that the number n of iterations is less than N, where N is defined by:

$$\frac{1}{N} = q\,(1 + \frac{|Zs|^2}{|r|^2}). \tag{9}$$

APPENDIX 2

SINGULAR VALUE DECOMPOSITION (SVD)

Applying SVD to a complex square matrix **Z** with coefficients z_{ij}, i, j = 1, 2 gives:

$$\mathbf{Z} = [\mathbf{v}_1\ \mathbf{v}_2] \begin{bmatrix} \mu_1 & 0 \\ 0 & \mu_2 \end{bmatrix} [\mathbf{u}_1\ \mathbf{u}_2]^H, \tag{1}$$

with $\mathbf{U}^H$ being the transposed complex conjugate of **U**. The μ_i, $|\mu_1| \geq |\mu_2|$ are the singular values of **Z** and $\mathbf{u}_i$, $\mathbf{v}_i$ are, respectively the i-th right and the i-th left complex singular vector, normalized by the scalar products $\mathbf{u}_i\mathbf{u}_j^* = \mathbf{v}_i\mathbf{v}_j^* = \delta_{ij}$, with δ_{ij} being the Kronecker symbol and $\mathbf{u}_i\mathbf{u}_i > 0$ (real), $\mathbf{v}_i\mathbf{v}_i > 0$ (real).

In our case, the vectors $\mathbf{u}_i$ ($\mathbf{v}_i$) correspond to particular states of the B- and T-field in frequency space, which by Fourier transformation can be brought back to the time domain. We thus obtain two elliptically polarized states at a frequency f given by the polarization direction α (β) and ellipticity e (h) defined by:

principal direction field B: $\alpha = \arctan\,(u^r_{1y} / u^r_{1x})$,
principal direction field T: $\beta = \arctan\,(v^r_{1y} / v^r_{1x})$,
ellipticity field B: $e = 1 - |\,u^r_1\,| / |\,u^i_1\,|$),
ellipticity field T: $h = 1 - |\,v^r_1\,| / |\,v^i_1\,|$),

where:

v^r = *real part (v)* u^r = *real part (u)*,
v^i = *imag. part (v)* u^i = *imag. part (u)*,

REFERENCES

Golub G.H. and Van Loan C.F.; 1983: *Matrix Computations.* John Hopkins Univ. Press. (1-642).

Jankowski J., Marianiuk J., Ruta A., Sucksdorff C., Kivinen M.; 1984: *Long-term stability of a torque-balance variometer with photoelectric converters in observatory practice.* Geophysical Surveys, **6**, 367-380.

Kao D.W. and Rankin D.; 1977: *Enhancement of signal to noise ratio in magnetotelluric data.* Geophysics, **42**, 103-110.

Kaufmann A.K. and Keller G.V.; 1981: *The magnetotelluric data sounding method.* Elsevier, 1-595.

Jones A.G.; 1988: *Static shift of magnetotelluric data and its removal in a sedimentary basin environment.* Geophysics, **53**, 967-978.

LaTorraca G.A., Madden T.R. and Korringa J.; 1986: *An analysis of the magnetotelluric impedance for three dimensional conductivity structures.* Geophysics, **51** , 1819-1829.

Myachkin V.I., Sobolev G.A., Dolinka N.A., Morozow V.N., Preobrazensky V.B.; 1972: *The study of variations in Geophysical fields near focal zones of Kamchatka.* Tectonophysics, **14**, 287-293.

Qian J.; 1984: *Regional study of the anomalous change in apparent resistivity before the Tangshan earthquake (M = 7.8, 1976) in China.* PAGEOPH, **122**, 901-920.

Slejko D., Carulli G.B., Carraro F., Castaldini D., Cavallin A., Doglioni C., Iliceto V., Nicolich R., Rebez A., Semenza E., Zanferrari A. e Zanolla C.; 1987. *Modello Sismotettonico dell'Italia Nord-Orientale.* C.N.R., G.N.D.T. Rendiconto N. 1, Ricci, Trieste, 82 pp.

Sobolev G.A.; 1975: *Application of the electric method to the tentative short term forecast of Kamchatka earthquakes.* PAGEOPH, **113**, 229-235.

Varotsos P. and Alexopoulos K.; 1984: *Physical properties of the variations of the electric field of the earth preceding earthquakes I.* Tectonophysics, **110**, 73-98.

Yamazaki Y.; 1975: *Precursory and coseismic resistivity changes.* PAGEOPH, **113**, 219-227.

Yee E. and Paulson K.V.; 1987: *The canonical decomposition and its relationship to other forms of magnetotelluric impedance tensor analysis.* Geophysics, **61**, 173-189.

Yee E. and Paulson K.V; 1987: *Canonical decomposition of the telluric transfer tensor.* Geophysics, **61**, 190-199.

Yungul S.H.; 1977: *The telluric methods in the study of sedimentary structures-A survey.* Geoexploration, **15**, 207-238.

Zadro M., Santero P., Ernst T., Jankowski J., Marianiuk J., Teisseyre R.; 1988: *A preliminary note on the telluric records in the Friuli seismic zone (North-East Italy).* Proceedings of "Seminar on the Prediction of earthquakes". Lisbon, Portugal, 14-18 November 1988, 1-25.

Zadro M., Ernst T., Jankowski J., Rozluski C.P., Teisseyre R.; 1990: *The magneto-telluric recordings from seismic zone, Friuli, North East Italy.* Tectonophysics, **180**, 303-308.